

GRB021004: Reverse Shock Emission

Shiho Kobayashi and Bing Zhang

*Dept. of Astronomy & Astrophysics and Dept. of Physics,
Pennsylvania State University, 104 Davey Lab, University Park, PA 16802*

ABSTRACT

We show that the re-brightening in the GRB 021004 optical afterglow light curve around ~ 0.1 day can be explained within the framework of the standard fireball model. The superposition of a forward and reverse shock emissions result in the peculiar behavior. With the standard values of parameters obtained in other afterglow observations, we can construct an example case in which theoretical estimates reasonably fit the broadband observations. Therefore, the peculiarity of the light curve might be a common feature in early gamma-ray burst afterglows.

1. introduction

The prompt localization of GRB 021004 by HETE II allowed the follow-up of the afterglow at very early time. Torii, Kato and Yamaoka (2002) observed the error box of the burst ~ 3.5 mins after the trigger, yielding upper limit around $R \sim 13.6$ mag. An optical transient at the level of $R \sim 15.56$ mag was detected, ~ 9 mins after the trigger, by the Oschin/NEAT robotic telescope (Fox 2002).

The dense sampling of the afterglow light curve at early time revealed the peculiarity, a major re-brightening around ~ 0.1 day after the trigger and a short time scale variability around ~ 1 day. The slope of the afterglow is $\sim t^{-0.69}$ for the earliest three observations (9-17 min after trigger) by the Oschin/NEAT robotic telescope, and after the luminosity increases around ~ 0.1 days, it decayed with $\sim t^{-1.05}$ as usual afterglows do.

These temporal features might be modelled by refreshed shocks (Zhang and Mészáros 2002). Recently, Lazzati et al. (2002) proposed a model in which the features are due to the interaction of the fireball with enhancements in the ambient medium density. In this Letter, we show that the major re-brightening around ~ 0.1 day can be explained within the standard fireball model. We propose that the reverse shock emission dominated the optical band at early times, leading to the observed peculiarity.

2. Observations

GRB 021004 triggered HETE II on 2002 October 4 at 12:06:13 UT. The burst lasted approximately $T \sim 100$ seconds (Shirasaki et al. 2002) and the fluence was $\sim 3.2 \times 10^{-6}$ ergs cm^{-2} in the 7 – 400 keV band (Lamb et al. 2002). The spectroscopic observations of the optical afterglow revealed an emission line interpreted as Ly- α at $z = 2.328$ (Mirabal et al. 2002). Then, assuming $\Omega_0 = 0.3$, $\lambda_0 = 0.7$ and $h = 0.6$, the isotropic gamma-ray energy is about 5.6×10^{52} ergs. The optical observations of the afterglow are depicted in Fig 1.

3. The model

We apply a standard fireball model to explain the re-brightening in the optical afterglow, in which a relativistic shell (fireball ejecta) with energy E , a Lorentz factor η and a width Δ_0 expanding into the homogeneous ISM with a particle number density n . When the shell sweeps a large volume of the ISM, it is decelerated and the kinetic energy is transferred to the ISM by shocks (e.g. Kobayashi, Piran & Sari 1999). The shocked ISM forms a relativistic blast wave (forward shock) and emit the internal energy via synchrotron process. Afterglows at late times is described by this forward shock emission well.

The emission from a reverse shock was also predicted (Mészáros & Rees 1997; Sari & Piran 1999a). When the reverse shock crosses the shell, the forward shocked ISM and the reverse shocked shell carry comparable amounts of energy. However, the typical temperature of the shocked shell is lower since the mass density of the shell is higher. Consequently, the typical frequency in the shocked shell is lower. A prompt optical emission from GRB 990123 (Akerlof et al. 1999) can be regarded as this emission (Sari & Piran 1999b; Kobayashi & Sari 2000). The early optical afterglow of GRB 021004 can be dominated by this reverse shock emission.

3.1. Forward Shock

Observations of optical afterglows usually start around several hours after the burst trigger. Since, at such a late time, the typical synchrotron frequency of the forward shock emission is lower than optical band, the evolution of afterglows is well described by a single power law, except for the jet break (Rhoads 1999; Sari, Piran & Halpern 1999).

However, an optical light curve is expected to have other breaks at early times. With reasonable values of parameters, say with $E = 10^{52}$ ergs, $n = 1$ proton cm^{-3} , $\epsilon_B = 0.01$

and $\epsilon_e = 0.1$ where ϵ_B and ϵ_e are the fractions of the shock energy given to magnetic field and electrons at the shock, the typical synchrotron frequency $\nu_{m,f}$ crosses the optical band $\nu_R \sim 5 \times 10^{14}$ Hz before the cooling frequency $\nu_{c,f}$ crosses it, and the optical light curve has a peak when $\nu_{m,f}(t) = \nu_R$ (see fig 2(b) in Sari, Piran and Narayan 1998). Before the peak time $t_{m,f}$, the luminosity increases as $\propto t^{1/2}$, and reaches to the maximum flux $F_{\nu,max,f}$, and then decays as $\propto t^{3(1-p)/4}$. p is the index of the power law distribution of random electrons accelerated at shock.

$$\nu_{m,f}(t) \sim 5.7 \times 10^{14} (1+z)^{1/2} \epsilon_B^{1/2} \epsilon_e^2 E_{52}^{1/2} t_d^{-3/2} \text{ Hz}, \quad (1)$$

$$\nu_{c,f}(t) \sim 2.7 \times 10^{12} (1+z)^{-1/2} \epsilon_B^{-3/2} E_{52}^{-1/2} n_0^{-1} t_d^{-1/2} \text{ Hz}, \quad (2)$$

$$t_{m,f} \sim 0.69 (1+z)^{1/3} \epsilon_B^{1/3} \epsilon_e^{4/3} E_{52}^{1/3} \nu_{R,15}^{-2/3} \text{ days}, \quad (3)$$

$$F_{\nu,max,f} \sim 1.1 \times 10^2 (1+z) \epsilon_B^{1/2} E_{52} n_0^{1/2} D_{28}^{-2} \text{ mJy}. \quad (4)$$

where $E_{52} = E/10^{52}$ ergs, $\nu_{R,15} = \nu_R/10^{15}$ Hz. $n_0 = n/1$ proton cm^{-3} , and here D_{28} is the luminosity distance in unit of 10^{28} cm, t_d is the observer's time in unit of day, $F_{\nu,max,f}$ does not depend on time.

Assuming that the re-brightening with the peak luminosity of ~ 1 mJy around ~ 0.1 day is caused by this peak, we get the following formulae for ϵ_e and n_0 as functions of ϵ_B and other known parameters. (The slope ~ -1.05 of the afterglow at late time means $p \sim 2.4$.)

$$\epsilon_e \sim 8.0 \times 10^{-2} \epsilon_B^{-1/4} \left(\frac{1+z}{3.3} \right)^{-1/4} \left(\frac{t_{m,f}}{0.1 \text{ day}} \right)^{3/4} \left(\frac{E}{5.6 \times 10^{52} \text{ ergs}} \right)^{-1/4} \left(\frac{\nu_R}{5 \times 10^{14} \text{ Hz}} \right)^{1/2} \quad (5)$$

$$n_0 \sim 5.1 \times 10^{-4} \epsilon_B^{-1} \left(\frac{1+z}{3.3} \right)^{-2} \left(\frac{F_{\nu,max,f}}{1 \text{ mJy}} \right)^2 \left(\frac{E}{5.6 \times 10^{52} \text{ ergs}} \right)^{-2} \left(\frac{D}{6.8 \times 10^{28} \text{ cm}} \right)^4 \quad (6)$$

3.2. Reverse Shock

We assume that the optical band is dominated by the reverse shock emission when the Oschin/NEAT robotic telescope observed the optical transient. The superposition of the forward shock emission and the reverse shock emission gives the initial decay of the afterglow.

The evolution of reverse shocks is classified into two cases (Kobayashi 2000). If the initial Lorentz factor of the shell η is larger than a critical value $\eta_c = (3E/32\pi n m_p c^2 \Delta_0^3)^{1/8}$ where m_p is the mass of proton, the reverse shock becomes relativistic in the frame of unshocked shell material during crossing the shell, and drastically decelerates the shell (thick shell case). If $\eta < \eta_c$, the reverse shock can not decelerate the shell effectively (thin shell case). According

to the internal shock model, the initial width of the shell Δ_0 is given by the intrinsic duration of the GRB $\sim cT/(1+z)$ (Kobayashi, Piran & Sari 1997).

$$\eta_c \sim 190 n_0^{-1/8} \left(\frac{1+z}{3.3} \right)^{3/8} \left(\frac{T}{100\text{sec}} \right)^{-3/8} \left(\frac{E}{5.6 \times 10^{52}\text{ergs}} \right)^{1/8}. \quad (7)$$

The shock crossing time and the Lorentz factor at that time are given by $t_\times \sim \max[t_{dec}, T]$ and $\gamma_\times \sim \min[\eta, \eta_c]$, respectively (Sari & Piran 1999a; Kobayashi 2000).

$$t_{dec} = (1+z) \left(\frac{3E}{32\pi\eta^8 n m_p c^5} \right)^{1/3} \sim 100 \left(\frac{1+z}{3.3} \right) n_0^{-1/3} \left(\frac{E}{5.6 \times 10^{52}\text{ergs}} \right)^{1/3} \left(\frac{\eta}{190} \right)^{-8/3} \text{sec}. \quad (8)$$

At the shock crossing time, the forward and reverse shocked regions have the same Lorentz factor $\gamma_\times = \min[\eta, \eta_c]$ and internal energy density e . Therefore, the cooling frequency $\nu_{c,r}$ of the reverse shock is equal to that of the forward shock $\nu_{c,f}$.

$$\nu_{c,r}(t_\times) \sim \nu_{c,f}(t_\times). \quad (9)$$

However, the typical frequencies are different. The mass density in the forward shock region is $\rho_f \sim e/\gamma_\times$, while one in the reverse shock region is $\rho_r \sim e/\bar{\gamma}_\times$ where $\bar{\gamma}_\times$ is the Lorentz factor of the shocked shell material in the frame of the unshocked shell material. Using a relation $\gamma_\times \bar{\gamma}_\times \sim \eta$, we get $\rho_r/\rho_f \sim \gamma_\times^2/\eta$, since the typical frequency of synchrotron emission is proportional to the electron's random Lorentz factor squared and to the magnetic field and Lorentz boost. The Lorentz boost and the magnetic field $\propto \sqrt{e}$ are the same for the two shocked regions, while the random Lorentz factor is proportional to η/γ_\times in the reverse shocked region and to γ_\times in the forward shocked region. Therefore, the reverse shock frequency at the crossing time (peak time) $\nu_{m,r}(t_\times)$ is given by (Sari & Piran 1999a)

$$\nu_{m,r}(t_\times) \sim \frac{\eta^2}{\gamma_\times^4} \nu_{m,f}(t_\times). \quad (10)$$

The peak flux at the typical frequency is proportional to the number of electrons and to the magnetic field and the Lorentz boost. From the energy conservation, the mass of the shell is larger by a factor of γ_\times^2/η at the crossing time than that of the ISM swept by forward shock. Since the number of electrons is proportional to the mass, we get

$$F_{\nu,max,r}(t_\times) \sim \frac{\gamma_\times^2}{\eta} F_{\nu,max,f} \quad (11)$$

Even though the hydrodynamic evolution of “thin” and “thick” shells is very different, the time dependence of the emissions are similar (Kobayashi & Sari 2000). If the optical

band ν_R is below the typical synchrotron frequency $\nu_{m,r}$ at the shock crossing time, the luminosity decreases as $\sim t^{-0.5}$. If $\nu_R > \nu_{m,r}$, it decreases as $\sim t^{-2}$ ($p = 2.4$) (Kobayashi 2000). Then, we have two choices for the time dependence of the reverse shock emission at the early time observations.

First we consider the case in which the reverse shock decreases as $\sim t^{-0.5}$. This means that the typical frequency of the reverse shock emission $\nu_{m,r}$ is above the optical band ν_R until the early observations $t_{m,r} \sim 0.01$ day by Oschin/NEAT telescope. The typical frequency of the forward shock emission crosses ν_R around $t_{m,f} \sim 0.1$ day. Then, we get a relation of $\nu_{m,r}(t_{m,r}) > \nu_R \sim \nu_{m,f}(t_{m,f})$. Since after the shock crossing, these typical frequencies decay with almost the same power law of $\sim t^{-3/2}$ (Kobayashi 2000), using eq. (10), we get

$$\eta > \gamma_{\times}^2 \left(\frac{t_{m,r}}{t_{m,f}} \right)^{3/4} \quad (12)$$

If GRB021004 is a thin shell case, $\gamma_{\times} \sim \eta$. The initial Lorentz factor is $\eta < 3$ for the standard parameters and too low to emit gamma-rays. If it is a thick shell case, we get $\eta > 6400$ for the standard parameters assumed in eq. (7). This might be too large, even though we can not reject the possibility that the central engine accelerates the shell to such a very high Lorentz factor.

Next we consider the case in which the reverse shock decreases as $\sim t^{-2}$ at the early observations around $t_{m,r} \sim 0.01$ day. For simplicity, we neglect the possibility that the typical frequency $\nu_{m,r}$ is above the optical band at the shock crossing time, but it crosses the optical band well before $t_{m,r}$. Assuming that $\nu_{m,r}$ is below the optical band at the shock crossing time, the reverse shock emission simply decreases as t^{-2} . Since the extrapolation of the light curve from the data points by Oschin/NEAT robotic telescope to the earlier time $T \sim 100$ sec $\sim 10^{-3}$ day with a power law of t^{-2} is not consistent with the upper-limits by Torii et al (2002) (see fig1), GRB 021004 should be a thin shell case. If so, the reverse shock emission peaks after their observations, or the peak is lower than their limits.

Using eqs. (5) and (6) with $t_{m,f} \sim 0.06$ days, $F_{\nu,max,f} \sim 1.3$ mJy, $E \sim 5.6 \times 10^{52}$ ergs, $z \sim 2.3$, $p \sim 2.4$, we search for a set of parameters (ϵ_B, η) with which the theoretical estimates give a reasonable fit to all observations. If we use a normalized Lorentz factor $\kappa \equiv \eta/\eta_c$ instead of η , we can show that the crossing time $t_{\times} \propto \kappa^{-8/3}$ and the optical flux from the reverse shock at the crossing time $F(t_{\times}) = (\nu_R/\nu_{m,r})^{-(p-1)/2} F_{\nu,max,r} \propto \kappa^p \epsilon_B^{(2-p)/8}$. Assuming the crossing time (peak time) $t_{\times} \sim 470$ sec, we get $\kappa \sim 0.55$. By fixing ϵ_B , the optical flux $F(t_{\times})$ (and the whole light curve) is determined. However, it depends on ϵ_B very weakly $\propto \epsilon_B^{-1/20}$ ($p = 2.4$). Therefore, ϵ_B is not well determined from the light curve, or equivalently, we can explain the peculiar behavior of the light curve with a wide range of ϵ_B . ($\epsilon_e < 1$ requires $\epsilon_B > 10^{-5}$.)

Fig 1 shows an example case in which $\epsilon_B \sim 3.0 \times 10^{-3}$ are assumed. This choice leads to $\epsilon_e \sim 0.23$, $n = 0.29$ proton cm^{-3} and $\eta \sim 120$, which are surprisingly typical values obtained in other afterglow observations (Panaitescu and Kumar 2002). The dashed and dashed dotted lines show the optical light curve of the reverse and forward shock emission, respectively. The thin solid line depicts the total flux. Around the peak time of the forward shock ~ 0.1 day, our estimate slightly deviates from the observations. However, in our estimate, we assumed a simplified synchrotron spectrum which is described by a broken power law. Since a realistic synchrotron spectrum is rounded at the break frequencies (Granot, Piran & Sari 1999), a more accurate estimate should give a light curve rounded at the break times (dotted line). The very small time scale variability of the light curve, which is prominent around ~ 1 day, might be produced by small scale ISM turbulence (Wang & Loeb 2000; Holland et al. 2002a; Lazzati et al 2002). The latest data point in Fig 1 is lower than the extrapolation with a scaling of $t^{-1.05}$. This might be a signature of the side expansion of the jet.

4. X-ray and Radio Afterglow

In this section, we assume the value of parameters with which we have shown the example case in the previous section, and estimate the x-ray and radio afterglows.

$$\epsilon_B = 3.0 \times 10^{-3}, \quad \epsilon_e = 0.23, \quad n = 0.29 \text{ proton cm}^{-3}, \quad \eta = 120, \quad E = 5.6 \times 10^{52} \text{ ergs.} \quad (13)$$

With these parameters, the break frequencies and the peak flux at the shock crossing time ~ 470 sec are given by

$$\nu_{m,f} \sim 1.8 \times 10^{16} \text{ Hz} \quad \nu_{c,f} \sim 1.8 \times 10^{17} \text{ Hz} \quad F_{\nu,max,f} \sim 1.3 \text{ mJy} \quad (14)$$

$$\nu_{m,r} \sim 1.2 \times 10^{12} \text{ Hz} \quad \nu_{c,r} \sim \nu_{c,f} \quad F_{\nu,max,r} \sim 1.6 \times 10^2 \text{ mJy.} \quad (15)$$

After the shock crossing, these evolve as $\nu_{m,f} \propto t^{-3/2}$, $\nu_{m,c} \propto t^{-1/2}$, $F_{\nu,max,f} = \text{const}$, $\nu_{m,r}, \nu_{c,r} \propto t^{-54/35}$ and $F_{\nu,max,r} \propto t^{-34/35}$ (Sari, Piran & Narayan 1998; Kobayashi 2000).

X-ray Afterglow: Since the X-ray band $\sim 5 \text{ keV} \sim 1 \times 10^{18} \text{ Hz}$ is well above the typical frequency of the reverse shock emission, the contribution from the reverse shock to the X-ray band is negligible. The x-ray afterglow should be described only by the forward shock emission. The luminosity in x-ray band should decrease as $t^{(2-3p)/4} \sim t^{-1.3}$ ($p = 2.4$). The Chandra x-ray observatory observed the afterglow for a total exposure of 87ksec, beginning at Oct 5 8:55 UT, 20.5 hours after the burst (Sako and Harrison 2002). The count rate decrease with time throughout the observation with a power law slope of -1.0 ± 0.2 . The mean 2-10 keV x-ray flux is $\sim 4.3 \times 10^{-13} \text{ ergs cm}^{-2} \text{ s}^{-1}$. We estimate the 5 keV flux at the

observational mean time $1.36 \text{ days} \sim 2.5 \times 10^{-13} \text{ ergs cm}^{-2} \text{ s}^{-1}$. Our estimates are in a good agreement with the observations.

Radio Afterglow: The forward shock emission in radio band $\sim 10 \text{ GHz}$ increases as $\propto t^{1/2}$ until the typical frequency reaches to the maximum $\sim 1 \text{ mJy}$ at $\sim 80 \text{ days}$ (dashed dotted line in fig2). The emission from the reverse shock (dashed line) decreases as $t^{-16/35}$ until the typical frequency $\nu_{m,r}$ crosses the radio band at $\sim 3 \text{ hours}$ after the burst, at which the flux is about $\sim 8 \text{ mJy}$. After that it decays as $\propto t^{-2}$. At low frequencies and early times, self absorption takes an important role and significantly reduces the flux. A simple estimate of the maximal flux (dotted line) is the emission from the black body with the reverse shock temperature (Sari & Piran 1999a; Kobayashi & Sari 2000). The thin solid line depicts the total flux. We plot measurements (circles) and upper-limits (triangles) also. Since the observations are done in various frequencies, we scaled the observed value to the expected value at 10 GHz by using a spectral slope of 1^{-1} . This burst also might cause a bright radio flare $\sim 0.8 \text{ mJy}$ around $\sim 0.38 \text{ day}$ as observed in GRB 990123. Unfortunately, all observations (or available data at this time) were done after the reverse shock emission had become negligible. Our estimates are consistent with the observations within a factor of 2.

5. Conclusions

We have shown that the early re-brightening of the GRB 021004 optical afterglow light curve can be explained within the standard fireball model. We propose that the reverse shock emission dominated the optical band at early times. The superposition of the forward and reverse shock emission produces the unusual light curve. Observations of optical afterglow usually start around several hours after the burst trigger. Since at such a late time the typical synchrotron frequency of the forward shock emission is lower than optical band, the light curve is well described by a single power law. The reverse shock emission in the optical band decreases very rapidly $\propto t^{-2}$ and when the cooling frequency crosses the optical band, it disappears. In a late time, the contribution from the reverse shock to the optical band is negligible. However, the swift localization of GRB 021004 by HETE II allowed the follow-up of the afterglow at very early time. This burst has so far the earliest detected

¹Berger et al. (2002a,b) reported an unusual spectral spectral slope $F_\nu \sim \nu$ between 8.5 GHz and 86 GHz from the observations with the VLA on October 10.17 UT, and claimed that the spectrum is not due to a transition from optically-thick (ν^2) to optically thin ($\nu^{1/3}$) emission. The superposition of the forward and reverse shock emission could give even flatter spectrum. Non-standard emission mechanism may be needed to explain this unusual spectrum.

optical afterglow. With the standard values of parameters inferred from other afterglow observations (Panaitescu and Kumar 2002), we have constructed an example case in which theoretical estimates fit the observations. We therefore suggest that such a peculiar behavior of the optical light curve might be a common feature in early afterglows. We have estimated the expected x-ray and radio afterglows with the parameters constrained by the optical observations. The results are consistent with the observations.

We would like to thank Peter Mészáros for valuable comments. We acknowledge support through the Center for Gravitational Wave Physics, which is funded by NSF under cooperative agreement PHY 01-14375, and through NSF AST0098416 and NASA NAG5-9192.

References

- Akerlof, C.W. et al. 1999, *Nature*, 398, 400.
Berger, E. et al. 2002, GCN 1613a.
Berger, E. et al. 2002, GCN 1613b.
Bersier, D. et al. 2002, GCN 1586.
Fox, D.W. 2002, GCN 1564.
Frail, D. & Berger, E. 2002, GCN 1574.
Granot, J., Piran, T. & Sari, R. 1999, *ApJ*, 527, 236.
Halpern, J.P. et al. 2002a, GCN 1578.
Halpern, J.P. et al. 2002b, GCN 1593.
Henden, A. 2002, GCN 1583.
Holland, S.T. et al. 2002a, *AJ*, 124, 639.
Holland, S.T. et al. 2002b, GCN 1585.
Holland, S.T. et al. 2002c, GCN 1597.
Kobayashi, S. 2000, *ApJ*, 545, 807.
Kobayashi, S., Piran, T. & Sari, R. 1997, *ApJ*, 490, 92.
Kobayashi, S., Piran, T. & Sari, R. 1999, *ApJ*, 513, 669.
Kobayashi, S. & Sari, R. 2000, *ApJ*, 542, 819.
Lamb, D. et al. 2002, GCN 1600.
Lazzati, D. et al. 2002, submitted to *A&A*, astro-ph/0210333.
Malesani, D. et al. 2002a, GCN 1607.
Malesani, D. et al. 2002b, GCN 1645.
Masetti, N. et al. 2002, GCN 1603.
Matsumoto, K. et al. 2002a, GCN 1567.
Matsumoto, K. et al. 2002b, GCN 1594.
Mészáros, P. & Rees, M.J. 1997, *ApJ*, 476, 231.
Mirabal, J. et al. 2002a, GCN 1602.
Mirabal, J. et al. 2002b, GCN 1618.

- Oksanen,A. et al. 2002a, GCN 1570.
Oksanen,A. et al. 2002b, GCN 1591.
Panaitescu,A. & Kumar,P. 2002, ApJ, 571, 779.
Pooley,G. 2002a, GCN 1575.
Pooley,G. 2002b, GCN 1588.
Pooley,G. 2002c, GCN 1604.
Rhoads,J.E. 1999, ApJ, 525, 737.
Sahu,D.K. et al. 2002, GCN 1587.
Sako,M & Harrison, F.A. 2002, GCN 1624.
Sari,R. & Piran,T 1999a, ApJ, 520, 641.
Sari,R. & Piran,T 1999b, ApJ, 517, L109.
Sari,R., Piran,T & Halpern,J.P. 1999, ApJ, 519, L17.
Sari,R., Piran,T & Narayan,R. 1998, ApJ, 497, L17.
Shirasaki,Y. et al. 2002, GCN 1565.
Stanek,K.Z. et al. 2002, GCN 1598.
Stefanon,M. et al. 2002, GCN 1623.
Torii,K., Kato,T. & Yamaoka,H. 2002, GCN 1589.
Uemura,M. et al. 2002, GCN 1566.
Wang,X. & Loeb,A 2000, ApJ, 535, 788.
Weidinger,M. et al. 2002, GCN 1573.
Winn,J. et al. 2002, GCN 1576.
Zhang,B.& Mészáros,P. 2002, ApJ, 566, 712.
Zharikov,S. et al. 2002, GCN 1577.

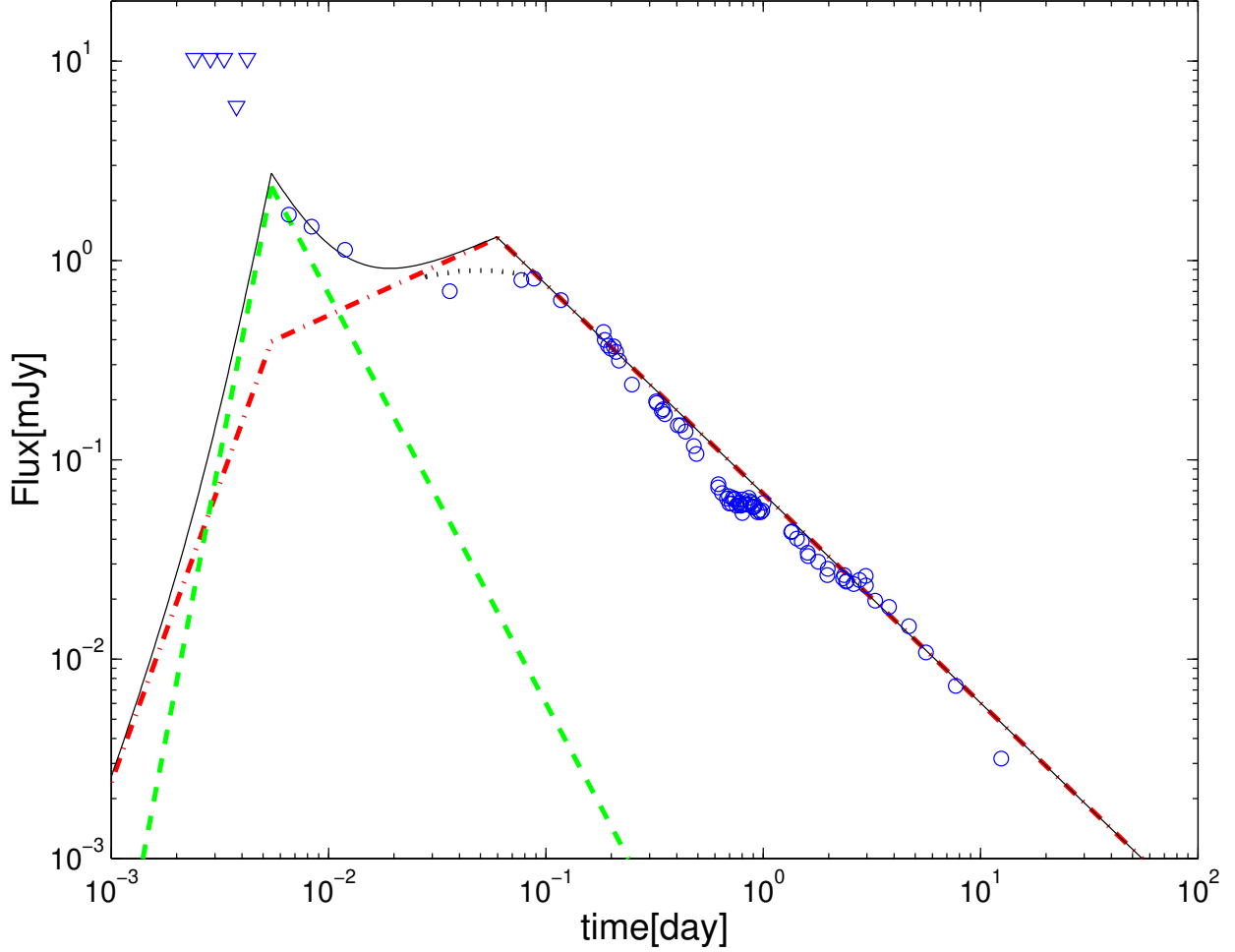


Fig. 1.— Optical light curve: forward shock emission (dashed dotted), reverse shock emission (dashed), total flux (thin solid), measurements (circles), upper-limits (triangles) and flux expected from accurate spectrum modelling (dotted). $E = 5.6 \times 10^{52}$ ergs, $\eta = 120$, $n = 0.29$ protons cm^{-3} , $\epsilon_B = 3.0 \times 10^{-3}$ and $\epsilon_e = 0.23$. Data from: Bersier et al. 2002; Fox 2002; Halpern et al. 2002a,b; Holland et al. 2002b,c; Malesani et al. 2002a,b; Masetti et al. 2002; Matsumoto et al. 2002a,b; Mirabal et al. 2002a,b; Oksanen et al. 2002a,b; Sahu et al. 2002; Stanek et al. 2002; Stefanon et al. 2002; Torii et al. 2002; Uemura et al. 1566; Weidinger et al. 2002; Winn et al. 2002; Zharikov et al. 2002, following the calibration of Henden 2002.

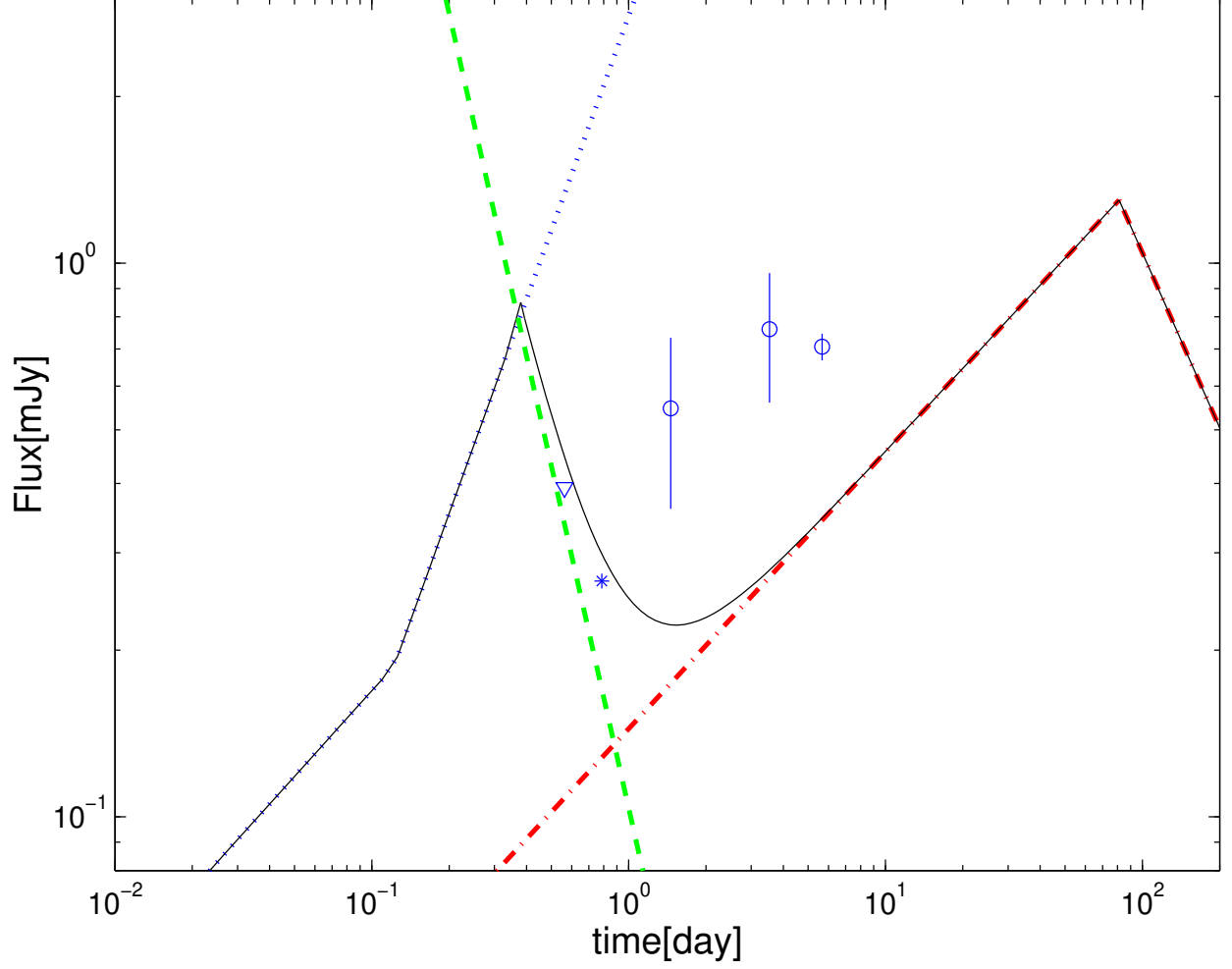


Fig. 2.— Radio light curve: forward shock emission (dashed dotted), reverse shock emission (dashed), self-absorption limit (dotted), total flux (thin solid). measurements with error bars (circles), measurement without error bar (star) and upper-limit (triangle). Data from: Frail & Berger 2002; Pooley 2002a,b,c; Berger et al. 2002b.